EMPIRICAL VALIDATION OF A TRANSIENT COMPUTER MODEL FOR COMBINED HEAT AND MOISTURE TRANSFER

Carsten Rode, Ph.D. **Douglas M. Burch**

ABSTRACT

A computer program for transient modeling of combined heat and moisture transfer in building constructions is introduced. The model's predictions are compared against moisture content and heat flux data obtained for six typical North American lightweight wall constructions that have been exposed to climatic conditions in a calibrated hot box. A special aspect of the work was that the basic moisture and thermal transport properties were determined for each individual material in the walls. The experiment, and thus the validation, was restricted to diffusive transport mechanisms taking place in the hygroscopic region.

Using the detailed information on the material properties, the program was able to predict the measured moisture content of the walls' siding and sheathing materials to within approximately 1% moisture content by weight, and the heat flows were predicted with a satisfactory accuracy. In a subsequent sensitivity analysis, the moisture transport properties were described as simpler functions or selected arbitrarily from a database of ordinary building materials. In some cases, this had a noticeable effect on the resulting moisture contents. It is suggested that transient heat and moisture transport models can be used in the design and analysis of constructions if the user is knowledgeable about the workings of such models and cautious in interpreting the results.

INTRODUCTION

History of Research Models for Combined Heat and Moisture Transfer

Models that predict the dynamic modes of coupled heat and moisture transfer in building constructions are not new inventions. As early as 1958, a simple scheme that calculated the transient distribution of moisture in a concrete roof was presented by Chlusov. Such calculations were done by hand.

A more theoretical basis for modeling the coupled transport phenomena in porous media was developed in the late 1950s with the work of Philip and de Vries (1957) and later Luikov (1966). These researchers presented models to calculate the combined heat and moisture transport by two governing partial differential equations using, as driving potentials, the moisture content and the temperature.

The transport coefficients in these models are nonlinear functions of the driving potentials. This fact, along with the lack of efficient solution techniques available when the theory was developed, meant that it was hardly possible to use the equations to predict the hygrothermal performance of building materials and structures for practical situations. The use of the equations was restricted to analytical studies of simplified cases and small-scale attempts at processing the equations numerically.

New measuring techniques provided the necessary raw data to determine the moisture transport coefficients for the above-mentioned transport models as functions of moisture content (van der Kooi 1971; Nielsen 1974). Most of this research was carried out in the laboratory to analyze the behavior of single materials.

Numerical implementation of the theoretical transport models evolved particularly in the early 1980s with the work of researchers such as Kießl (1983) and Kohonen (1984). Their efforts helped the theory to be applied in more practical situations by analyzing composite building structures exposed to realistic indoor and outdoor climatic conditions. The main objective of these numerical models was to use them for research purposes.

Today, research produces still more developed simulation tools that are now often multidimensional, complete heat, air, and moisture transport models. A recent overview of existing simple and advanced models is given by Hens and Janssens (1993).

Carsten Rode is a senior researcher with the Danish Building Research Institute, Hørsholm, Denmark. **Douglas M. Burch** is a research mechanical engineer at the Building and Fire Research Laboratory, National Institute of Standards and Technology, Gaithersburg, Md.

Thermal Performance of the Exterior Envelopes of Building VI, Conference Proceedings,

Evaluation Methods Used in Practice

Building designers have had mainly two options to use for moisture-related design of building structures:

- either use guidelines or codes of practice published nationally or
- predict the moisture conditions based on a steady-state calculation method, sometimes referred to as Glaser's method (Glaser 1959), or ASHRAE's vapor pressure/saturation vapor pressure intersection method (ASHRAE 1993).

Guidelines and codes of practice are valuable tools for the design of common construction types. However, they fall short when innovative designs, materials, or unusual indoor or outdoor climatic conditions occur.

The steady-state calculation method has a number of deficiencies in the way it is usually applied.

- The method does not consider the moisture capacity of the building materials.
- Diffusion is the only transport mechanism considered.
- Transport properties are assumed constant, which, in many cases, is not valid for vapor permeability.
- Boundary conditions commonly used are too simplistic. That is, constant mean values of air temperature and relative humidity are used on both sides of the construction, while solar and longwave radiation are seldom considered.

Thus, there is a need for reliable prediction tools that can be used in practice to evaluate new designs of building structures or to aid in modifying an existing design.

Practical Models of Today

Over the past five years, a number of practical simulation tools have been developed that run on personal computers, are easy to use, and have attached databases containing properties for the most common building materials (Pedersen 1990; Burch and Thomas 1994; Künzel 1994).

At issue is how well such models perform. This is a twofold question: (1) Are the models validated to predict with reasonable accuracy the processes they simulate? (2) Do the models take all relevant processes into account?

This paper focuses mainly on the first of these two questions. In addition, an investigation was performed to determine the sensitivity of the predicted results to the function used to represent the water-vapor permeability. In practice, various approximations are used to represent the water-vapor permeability.

The use of sufficient models to analyze certain cases is also very important but beyond the scope of this paper. For instance, in applications where convective heat and moisture transfer prevails, models that consider only the diffusive mechanisms may fail completely.

For the coupled transport phenomena dealt with by the type of models discussed in this paper, validation can be carried out in three ways:

1. By testing against situations for which analytical solutions exist—Probably all models have gone through some of this, but it cannot be done for complex situations that resemble real circumstances with composite structures composed of materials with highly variable transport properties and varying boundary conditions.
2. By comparing against a reference model—However, a single reference model does not exist and may also, in the future, be hard to establish in the field of combined heat, air, and moisture transport.
3. Empirical validation with experimental data—The problem here is that, although a large number of laboratory and field tests have been carried out, not many of these have specifically targeted *both* the elemental properties of the materials *and* the performance of the composite structures in which the materials function.

This paper demonstrates the use of the empirical approach. As in this paper, most empirical validations are only partial since not all the processes that can be simulated with a program are also investigated in the experiments, or the experiments do not cover the full range of possible variation of the important variables.

The Simulation Program

The program being used for analysis in this paper was originally developed as part of a Ph.D. project (Pedersen 1990). This program has been used to analyze the hygrothermal performance of constructions with hygroscopic materials in a number of research projects (e.g., Pedersen et al. [1992], Kyle and Desjarlais [1994]), and IEA Annex 24 [Hens and Janssens 1993]). The program is also being used by some building designers and manufacturers of building products.

Basic Transport Equations Used

The basic transient transport equations used in the program are given below.

For calculation of the temperature distribution:

$$\rho c \frac{\partial T}{\partial t} = \frac{\partial}{\partial x}\left(k \frac{\partial T}{\partial x}\right) + \Delta h_v \frac{\partial}{\partial x}\left(\delta_p \frac{\partial p_v}{\partial x}\right). \quad (1)$$

For calculation of the moisture distribution:

$$\rho \frac{\partial u}{\partial t} = \frac{\partial}{\partial x}\left(\delta_p \frac{\partial p_v}{\partial x}\right) + \frac{\partial}{\partial x}\left(K \frac{\partial P_l}{\partial x}\right) \quad (2)$$

where

ρ = density of the material, kg/m^3 (lb/ft^3);

c = specific heat of the material, J/(kg·K) (Btu/[lb·°F]);
T = temperature, K (°F);
x = one-dimensional space coordinate, m (ft);
k = thermal conductivity, W/(m·K) (Btu·in./[h·ft²·°F]);
Δh_v = phase conversion enthalpy, water vapor J/kg (Btu/lb);
δ_p = water vapor permeability, kg/(m·s·Pa) (gr·in./[h·ft²·in. Hg]);
p_v = water vapor pressure, Pa (in. Hg)
u = moisture content, mass of moisture by dry mass of the material, kg/kg (lb/lb);
K = hydraulic conductivity, kg/(m·s·Pa) (gr·in./[h·ft²·in. Hg]); and
P_l = capillary water pressure, Pa (in. Hg).

In these equations, the most important way in which the temperature distribution affects moisture flow is through its influence on the vapor pressure distribution.

Implementation

Equations 1 and 2 have been implemented in the program using a control volume method with finite-difference approximations of the partial derivatives and are solved using an implicit calculation scheme. This scheme is numerically stable and is solved without iterating between the equations, using time steps of typically one hour. However, in order to limit the excursion during one time step of those variables that determine the material properties, the program has some built-in routines to allow only a certain maximum excursion of the variables. This may cause the program to divide a time step into smaller fractions when necessary. The reader is referred to Pedersen (1991) for more detailed issues on how the two basic equations have been implemented.

All in all, the program allows for an expedient solution of the governing equations. The program contains a database of parameters that describes how the material properties vary with temperature and, more important, with moisture content. The properties are expressed in a number of empirical expressions of varying complexity that describe the wide range of variation. However, it is also possible to input the property data in tables of variable length. Thus, the properties can be described with varying levels of specificity. The importance of how well the properties are described will be discussed later in the paper for one of the constructions to be analyzed.

The program normally predicts the hygrothermal performance of wall or roof assemblies that separate an indoor climate from the outdoors. The indoor climate is described simply by monthly values for air temperature and humidity: either a relative humidity or a vapor concentration difference between indoor and outdoor air. The outdoor climate is typically read from a weather file and comprises such data as dry-bulb temperature, humidity, solar radiation, and wind speed, and it is possible to consider driving rain as a moisture source for the outermost control volume. Both indoor and outdoor conditions can also be read directly as hourly values from a file, as has been done in this work where the experimental boundary conditions will be simulated.

The program considers the transfer of latent heat that takes place when water evaporates at one location in a construction, is transferred as vapor, and condenses at another location. For constructions with permeable materials and under certain exposures, this form of enthalpy flow may be as important as thermal conduction. An analysis of this phenomenon has been carried out by Pedersen and Courville (1991).

Validation Work

Since the program is available for use by researchers and building designers, there is a continuing need to collect and disseminate information on any partial verification with complex and well-described experiments. This paper is an attempt to do just that. The author of the program previously has carried out other partial verifications of it (Pedersen 1990; Pedersen et al. 1992), so the justification of the work described in this paper lies in the rare opportunity to test the program against a complete set of experimental data for composite wall constructions where the properties of the individual wall materials are also well known.

This verification is only partial since it is restricted to conditions in the hygroscopic region. Moisture transfer in the experiment described in the next section took place at humidity levels and through materials where liquid moisture flow played essentially no role, e.g., the moisture content of the wooden parts stayed mainly below fiber saturation. A verification of the program's ability to consider liquid moisture flow has been shown earlier by Pedersen (1990) for drying of initially saturated aerated concrete.

It should be stated that this validation does not intend to test the program's ability to simulate exposure to rain, wind, or stack pressures, as these effects were not simulated in the experiment. The model is able to consider these effects only partially, e.g., rain is approximated as a moisture source in the most exterior control volume, and airflow can be considered only as one-dimensional filtration. Users should keep that in mind when selecting their tool for analysis.

DESCRIPTION OF WALL EXPERIMENTS

This section summarizes a comprehensive set of experiments conducted to obtain an accurate set of measurements to verify models that predict the combined transfer of heat and moisture in building envelopes. A more complete description of the experiment is given in Zarr et al. (1995).

Overview

Six different multilayered wall specimens were built and assembled collectively in a calibrated hot box (Zarr et al. 1987). The hot box provided controlled temperature and relative humidity conditions at the interior and exterior surfaces of the wall specimens. The wall specimens were first preconditioned to provide initial moisture contents in their construction materials. In the subsequent test period, the exterior surfaces of the wall specimens were exposed to a sequence of winter conditions that caused moisture to permeate into the wall specimens and accumulate in the exterior construction materials as a function of time. This was followed by a period with warm outside conditions that caused the exterior construction materials to lose moisture back to the interior environment. The moisture content of the exterior construction materials and the inside surface heat flux of the wall specimens were measured and will be compared to corresponding values predicted by the calculation program.

Wall Specimens The construction details of the six wall specimens analyzed in this paper are given in Figure 1. Each wall specimen had overall dimensions of 1.0 by 1.1 m (3.3 by 3.6 ft) and was installed in the calibrated hot box. Each wall specimen contained a center circular metering section circumscribed by a thin 0.03-mm (0.001-in.) plastic sleeve that minimized lateral moisture flow and provided one-dimensional moisture transfer within the metering section. A finite-difference analysis was conducted and revealed that the heat transfer within the metering area was also one-dimensional.

Calibrated Hot Box The metering chamber of the calibrated hot box provided a downward airstream at the interior surface of the wall specimens that was maintained at 21.2°C ± 0.1°C (70.2°F ± 0.2°F) and 50% ± 3% RH during the entire experiment. The climatic chamber of the calibrated hot box generated an upward airstream at the exterior surface of the wall specimens. The temperature of the climatic chamber during the test period is summarized in Table 1 and plotted in Figure 2. Its humidity was maintained at 5% ±3% RH during the test period.

Instrumentation

The metering section of each wall specimen was instrumented as shown in Figure 3a. The ambient temperature was measured at a distance of approximately 50 mm (2 in.) from the inside and outside surfaces of the wall specimens. The heat flux was measured at the interior surface of the gypsum board. The moisture content and surface

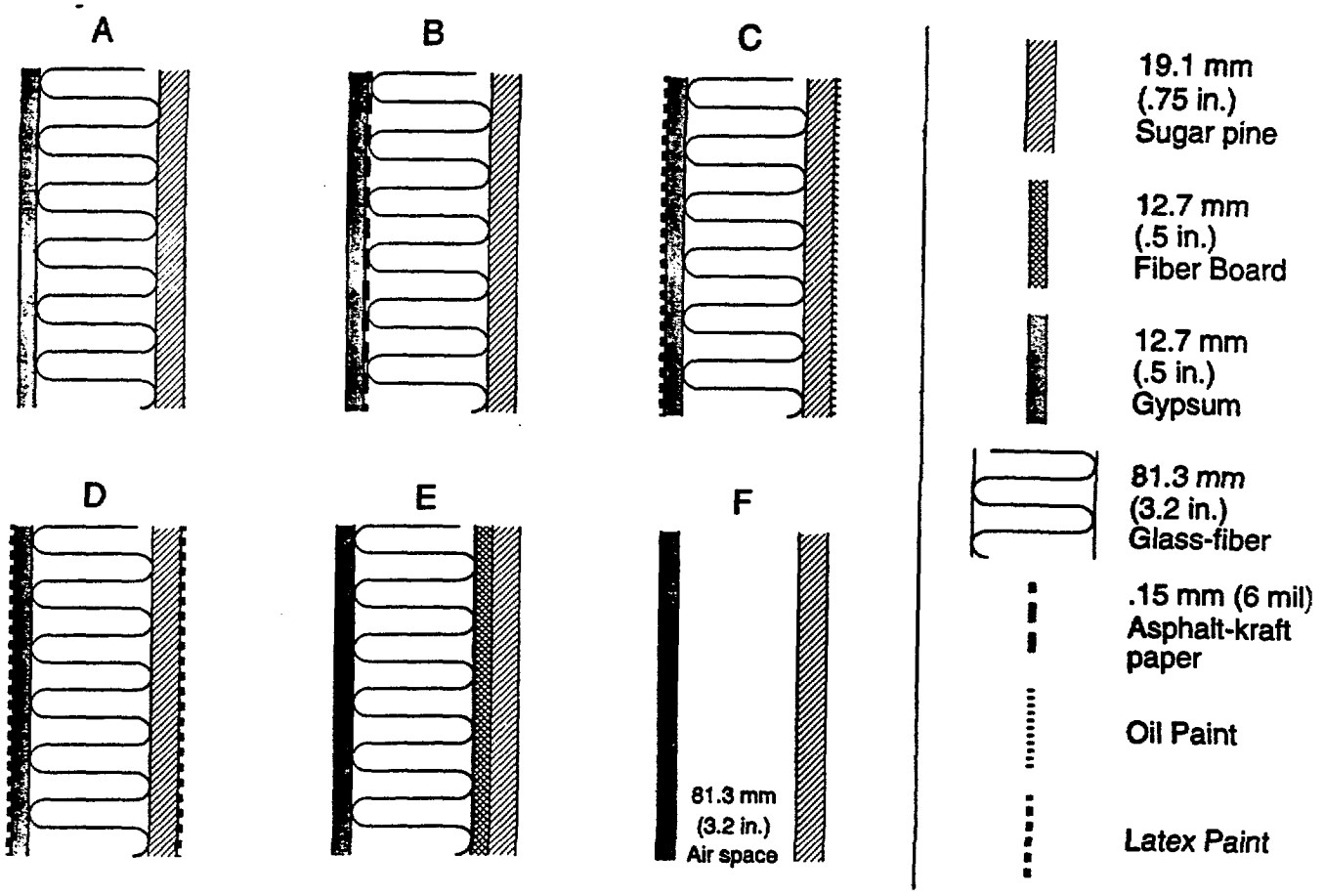

Figure 1 Wall layouts tested in the experiment. The left-hand side of all constructions faces the metering chamber (indoor conditions) and the right-hand side, the climate chamber (outdoor conditions).

TABLE 1 Climate Chamber Conditions

Condition	Days	Temperature (± Amplitude) (°C)	(°F)
Winter—Steady	1	7.2	45
Winter—Diurnal Sinewave	6	7.2 ± 8.0	45 ± 14
Winter—Steady	34	7.2	45
Winter—Diurnal Sinewave	7	7.2 ± 8.0	45 ± 14
Summer—Steady	14	32.2	90

The sinewaves had a period of one day. The temperature varied within an approximately ± 0.3 °C (± 0.5 °F) band during the periods with steady exposure (an outage excepted).

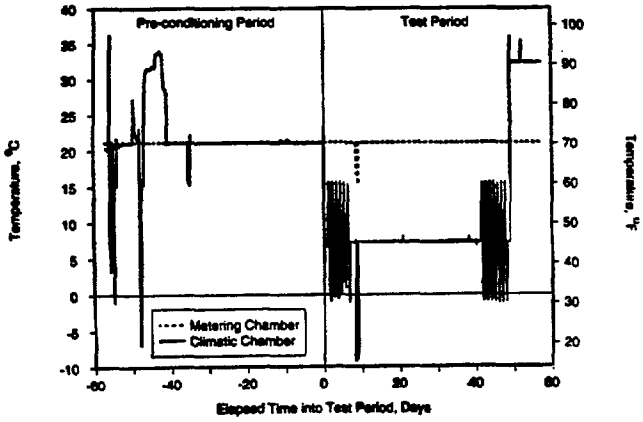

Figure 2 Thermal boundary conditions during the wall experiment. The average relative humidity during the test period was around 5% in the climate chamber and 50% in the metering chamber.

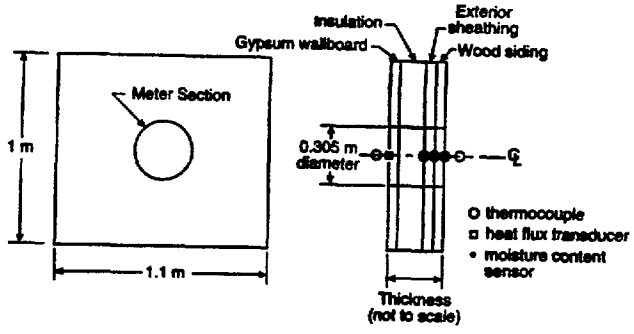

a. Wall specimen sensor location

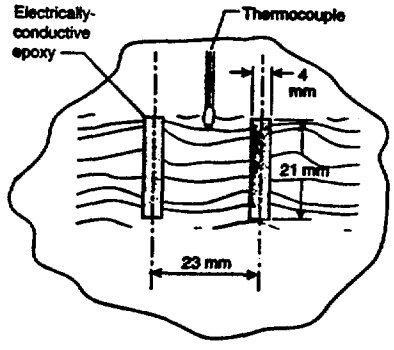

b. Construction of moisture content sensor

Figure 3 Description of instrumentation.

temperature were measured at the interior surface of the sheathing (if present) and both the interior and exterior surfaces of the sugar pine.

The ambient relative humidity was measured at the center of the airstreams on opposite sides of the wall specimens using calibrated capacitance-type relative humidity transducers. Calibrated thermocouple wire was used for the temperature measurements. Details relating to the moisture content and heat flux measurements are given below.

Moisture Content The moisture content of the wood-based materials was measured using the electrical-resistance method (Duff 1968). This method is based on the principle that, below fiber saturation, there exists a unique relationship between moisture content and electrical resistance for different species of wood and other building materials. For this experiment, a commercial moisture meter with a display resolution of 0.1% moisture content was used. The two-pin metal electrodes supplied with the meter were replaced with a pair of parallel electrically conductive epoxy strips applied to the surface of the wood-based materials (see Figure 3b).

After the experiment, the moisture content sensors were individually calibrated. This was accomplished by removing the sensors from their corresponding wall specimen with a 100-mm by 100-mm (4-in. by 4-in.) section of the substrate material. The sensors were then placed inside a precision temperature and humidity chamber that conditioned the substrate materials to various moisture contents at ambient temperatures of 4.4°C (39.9°F) and 32.2°C (90.0°F). For each sensor, the relationship between the metered moisture content and the actual moisture content was established at the two ambient temperature conditions. During the calibrated hot box experiment, the effect of temperature on the moisture content measurements was included by linear interpolation between the two reference calibration curves.

Heat Flux The heat flux at the center of the metered section of each of the wall specimens was measured using small heat flux transducers attached to the gypsum board using a silicone-rubber adhesive. The transducers were 23 mm (0.91 in.) in diameter and 3 mm (0.12 in.) thick. These heat flux transducers generated a millivolt signal directly proportional to the magnitude of the heat flux passing through the transducer. The heat flux transducers were calibrated by exposing them to heat fluxes in the guarded hot plate and establishing a relationship between millivolt output and heat flux.

Material Property Measurements

The material properties for the wall specimens were independently measured and input to the calculation model in order to minimize uncertainties associated with material variability. The property measurements included sorption isotherm measurements, permeability measurements, and thermal conductivity measurements

and are summarized below. Further information on the property measurements is given in Zarr et al. (1995).

Sorption Isotherm Measurements The sorption isotherms were determined by placing eight small specimens of each hygroscopic material in vessels above saturated saltwater solutions. Each saturated saltwater solution provided a fixed relative humidity (Greenspan 1977). The vessels were maintained at a temperature of 24°C ± 0.2°C (75°F ± 0.4°F) until the specimens reached steady-state equilibrium. The equilibrium moisture content was plotted vs. relative humidity to give the sorption isotherm. Separate sorption isotherm data were obtained for specimens initially dry (adsorption isotherms) and for specimens initially saturated (desorption isotherms). A detailed description of this measurement method is given in Richards et al. (1992).

The mean of the absorption and desorption isotherm measurements was fit to an equation of the form

$$u = \frac{B_1\phi}{(1+B_2\phi)\,(1-B_3\phi)} \qquad (3)$$

where ϕ = relative humidity.

The coefficients B_1, B_2, and B_3 were determined by regression analysis and are summarized in Table 2.

TABLE 2 **Sorption Isotherm Regression Coefficients**

Materials	B_1	B_2	B_3
Fiberboard sheathing	1.14	50.6	0.923
Glass-fiber insulation	0.00170	1×10^{-8}	0.963
Gypsum wallboard	0.00336	1×10^{-8}	0.901
Kraft paper with asphalt mastic	51.9	2538	0.902
Sugar pine	0.192	2.05	0.765

The uncertainty in the sorption isotherm measurements was within ±2.5% moisture content.

TABLE 3 **Vapor Permeability Regression Coefficients**

Materials	C_1	C_2	C_3
Fiberboard sheathing	-24.054	-.1004	0.0
Glass-fiber insulation	-22.425	0.0	0.0
Gypsum wallboard	-23.475	0.0	0.0
Kraft paper with asphalt mastic	-32.239	-1.168	3.058
Sugar pine	-28.677	-0.9198	4.576

TABLE 4 **Permeance of Paints**

Materials	Permeance (10^{-12} kg/s·m²·Pa)
Interior latex paint	980
Exterior latex paint	190
Exterior oil-base paint	80

The uncertainty in measuring the permeance of the materials was less than 5% when measuring materials having a permeance less than 5.7×10^{-10} kg/s·m²·Pa (10 perm). However, the uncertainty increased rapidly as the specimen permeance rose above 5.7×10^{-10} kg/s·m²·Pa (10 perm).

Permeability Measurements The water-vapor permeability of the rigid hygroscopic materials was measured using permeability cups placed in controlled environments. Five circular specimens, 140 mm (5.5 in.) in diameter, of each material were sealed at the top of open-mouthed glass dishes. The dishes were subsequently placed inside sealed glass vessels maintained at a constant temperature. Saturated salt-in-water solutions were used inside the glass dish and surrounding glass vessels to generate a relative humidity difference of approximately 10% across each specimen. By using different salt solutions, the mean relative humidity across the specimen was varied from a "dry" to a saturated state. Permeability was plotted vs. the mean relative humidity across the specimen. Separate measurements conducted at 7°C (45°F) and 24°C (75°F) revealed that temperature has only a small effect on permeability over this temperature range. A detailed description of the permeability measurement method is given in Burch et al. (1992). It is worth mentioning that the materials used in the wall experiment experience temperatures somewhat outside the range of the permeability measurements.

Vapor permeability data were plotted vs. the mean relative humidity across the specimen and fit to an equation of the form

$$\delta_p = \exp(C_1 + C_2\phi + C_3\phi^2). \qquad (4)$$

The coefficients C_1, C_2, and C_3 were determined by regression analysis and are summarized in Table 3.

The permeance of glass-fiber insulation was assumed to be equal to measurements of the permeability of a stagnant air layer. This assumption is reasonable because the glass fibers of the insulation occupy a very small fraction of its volume. In this situation, bound-water diffusion along the glass fibers is small compared with molecular diffusion through the predominantly open pore space. The permeances of the paint layers are given in Table 4.

Heat Transfer Properties The thermal conductivities of the materials were measured in accordance with ASTM Test Method C 177 (ASTM 1993) using the guarded hot plate. Each measurement was carried out at approximately the same mean temperature that the material experienced during the steady-state winter conditions of the experiment. The thermal conductivity of the glass-fiber insulation was determined at the same thickness and density as in the wall cavities. The densities of the materials were measured, and their specific heats were taken from ASHRAE (1993). The heat transfer properties for the materials are summarized in Table 5.

TABLE 5 Heat Transfer Properties of the Materials

Materials		Density (kg/m³)	Specific Heat (J/kg·K)	Thermal Conductivity (W/m·K)
Fiberboard Sheathing		380.4	1300	0.0539
Gypsum Wallboard		628.6	1090	0.159
Kraft paper with asphalt mastic		839.3	1256	0.159
Sugar Pine		373.8	1630	0.0865
Glass-fiber Insulation	Wall A	9.1	805	0.0445
	Wall B	9.2	805	0.0443
	Wall C	10.4	805	0.0426
	Wall D	6.0	805	0.0542
	Wall E	8.8	805	0.0450

The density of the glass-fiber insulation was determined by extracting an in-situ core sample of the insulation in line with the heat flux transducer. The thermal conductivity was subsequently calculated from a conductivity versus density correlation. The uncertainty in measuring the thermal conductivity was less than 1%.

VALIDATION EXERCISE

Input for the Calculations

Input files for the computer model were created for each of the six walls to best represent the situation in the experiment. The material properties were set up in tables typically using 14 points to describe how the equilibrium moisture content and the vapor permeability are functions of relative humidity. Each of these points was determined on the basis of Equations 3 and 4 and the constants in Tables 2 and 3. Values of simpler properties, such as dry density, heat capacity, and thermal conductivity, were taken directly from Table 5 and specified as constants for each of the materials. The same goes for the vapor permeances of paints (Table 4).

In the experiment, air speeds along the faces of the constructions were known in both the climate and metering chambers, so the convective heat transfer coefficients could be determined. Values for the radiative heat transfer coefficients were found from standard algorithms for the actual test conditions. These two coefficients were combined to give an overall heat transfer coefficient for each face that was used in the calculations. Moisture transfer coefficients for the two sides were found using the Lewis relation (Threlkeld 1970) between the convective heat and mass transfer coefficients.

The air space in wall F was simulated as single thermal and vapor diffusion resistances. The thermal resistance was taken from ASHRAE (1993) for two plane surfaces under conditions similar to those in the experiment. The vapor resistance was found, again using the Lewis relation, assuming the convective part of the thermal resistance was 0.5 $m^2 \cdot K/W$ (2.8 $ft^2 \cdot h \cdot °F/Btu$) and the Lewis number was 0.93. Table 6 summarizes the overall thermal and vapor resistances used for the outer surfaces and for the interior air space.

TABLE 6 Resistances for Exterior and Interior Air Layers

Layer	Overall Thermal Resistance ($m^2 \cdot K/W$)	Vapor Resistance ($GPa \cdot m^2 \cdot s/kg$)
Climate chamber surface	0.11	0.039
Interior air space (Wall F)	0.17	0.047
Metering chamber surface	0.12	0.069

To simulate the walls, a numerical mesh had to be set up for the construction. Twenty-nine control volumes with thicknesses between 0.23 mm (0.009 in.) and 28 mm (1.1 in.) were used to describe each of the walls A through E. Grid spacing was chosen to be finest for the sugar pine layer, where the moisture content gradients were expected to be highest. One of the main objects for comparison was the surface moisture content of the siding and sheathing of the wall specimens. Since this was measured at the inside of the layers, the grid was made such that the moisture contents of the inner 3.2 mm (1/8 in.) could be separately predicted.

Climatic files for the program were constructed using as input the measured boundary conditions in the two chambers. As initial conditions for the calculations, the measured moisture contents were used when the preconditioning period began. The simulations comprise both the preconditioning and test periods, although results will be shown only for the latter.

Comparison of Moisture Contents

Figure 4 shows for all six wall assemblies the measured and predicted moisture contents for the siding and for the sheathing in wall E. For each compared set of data, the root-mean-square difference between the measured and predicted results is indicated in the legend of the figure. This was calculated according to the following equation:

$$\mathrm{RMS} = \sqrt{\sum_{i=1}^{n} \frac{\left(u_{i,\,predicted} - u_{i,\,measured}\right)^2}{n}}. \qquad (5)$$

As can be seen from Figure 4, there is a fine correspondence between measured and predicted moisture contents with root-mean-squared differences around 1% moisture content by weight for all wall specimens. Thus, for the type of wall constructions tested in the experiment and the conditions under which the experiment was run, e.g., that it was restricted to the hygroscopic regime, the predictive model seems to be a valid tool with which to predict hygrothermal behavior. However, there are small deviations that are discussed below.

Close inspection of Figure 4 reveals that such deviations can either be seen as scaling errors during the whole or part of the test period (predominantly walls C, E, and F) or errors in the rate at which moisture is taken up or released (mainly walls A, B, and D).

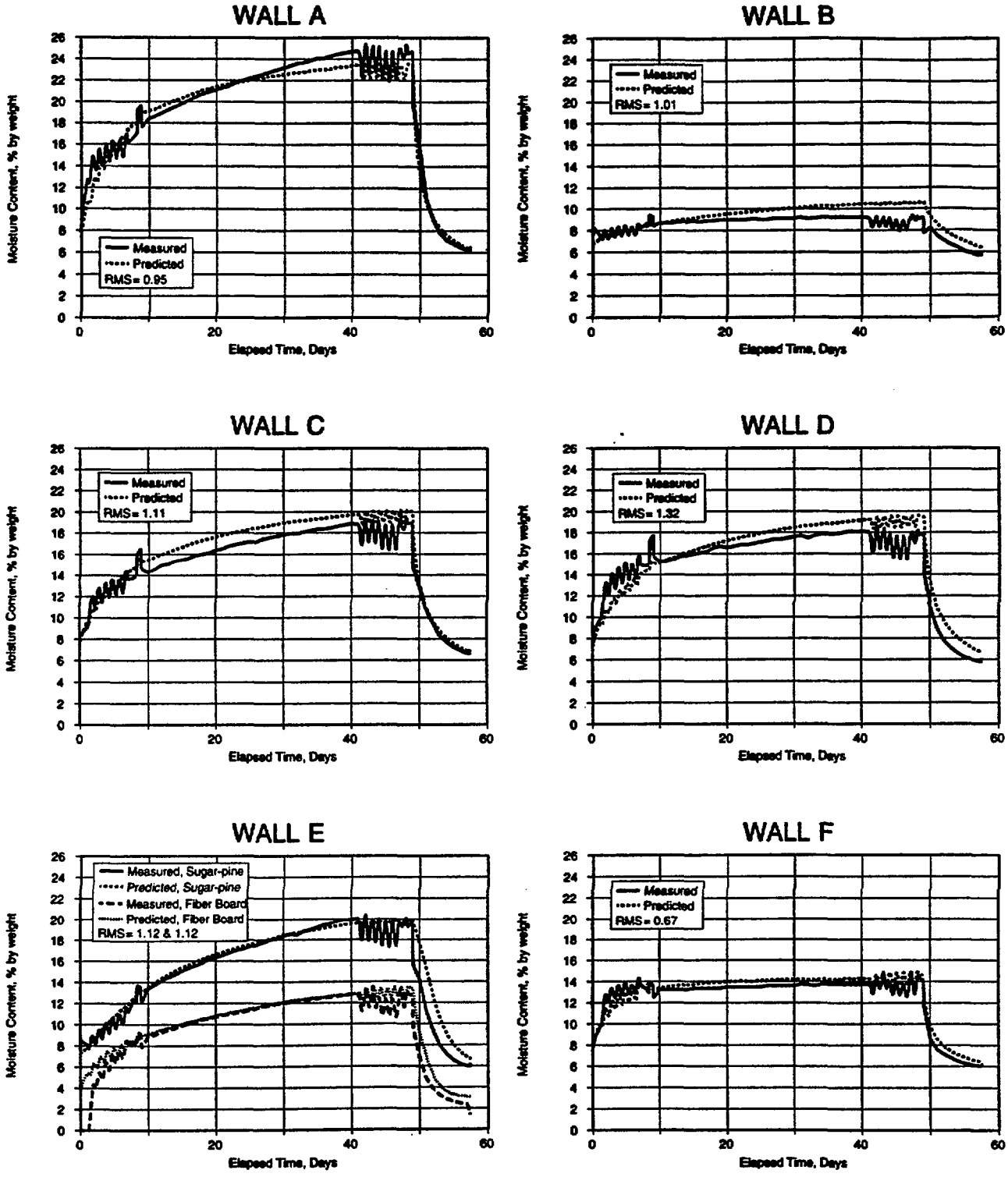

Figure 4 *Comparison of measured and predicted moisture contents of inside 3.2 mm (1/8 in.) of sugar pine siding for all walls and inside 3.2 mm (1/8 in.) of fiberboard sheathing of Wall E.*

The most important deviation is probably that the calculated moisture uptake rate of the sugar pine siding in wall A during the period with steady boundary conditions is only about two-thirds of the measured rate. However, the sugar pine is exposed to rather extreme conditions, with 5% RH on one side and about 90% on the other side. This causes large gradients in vapor permeability across the board that can be difficult to predict with high accuracy.

Another noticeable difference in moisture uptake rate can be seen for wall B, where the measurements show an almost constant moisture content throughout the period with steady boundary conditions. The most probable cause for this is an uncertainty in the measured vapor diffusion resistance of the asphalt-kraft paper. This is the only wall being tested where there is a significant vapor resistance on the warm side of the insulation, i.e., a layer that functions as a vapor retarder.

Comparison of Heat Flow Rates

For wall A, Figure 5 shows the measured and predicted heat flow rates at the interior surface throughout the entire test period. Although the program calculates latent as well as sensible heat flows, only the sensible part is presented in the figure. The reason is that, according to experience from another experimental project (Pedersen et al. 1992), it is not possible to measure the flow of latent heat with the kind of vapor-impermeable heat flux transducers that were used in the experiment positioned on the surface of a permeable or hygroscopic material. The hypothesis is that some of the vapor that would expectedly have condensed on the transducer and caused it to give a higher signal when the condensation heat was released is instead diverted by the hygroscopic attraction of the materials around the transducer.

The two periods of dynamic boundary conditions close to the beginning and end of the test period are clearly discernible from the heat flow pattern with the steady-state period in between. As far as can be seen from this figure, the predicted and measured results track each other reasonably well, but the time scale and fluctuation of data do not allow this to be seen with sufficient detail.

Figure 6 shows the average measured and predicted heat flow for all wall specimens for the steady-state period. The discrepancies vary between 0.8% and 9.1%. The largest deviation is for wall F, with an empty airspace instead of an insulation layer. The thermal resistance of this layer was not measured for this assembly in particular, and that may be the main cause of the large deviation. For the other walls, the discrepancy is up to 7.6% and may either be positive or negative.

Figure 7 shows the results for all six walls for one of the dynamic periods. Again, prediction and measurement track each other well, with RMS values up to around 0.7 W/m^2 (0.22 Btu/h·ft^2) for walls A through E. Uninsulated wall F has a much larger RMS value of 1.5 W/m^2 (0.47 Btu/h·ft^2), which is first of all due to the generally higher level of heat flux but is also due to the uncertainty about the insulation value of the airspace.

It is believed that a major cause of deviation between measured and predicted heat fluxes of the insulated walls could be uncertainty in the local in-situ insulation density, which has an important effect on the thermal conductivity (see Table 5). With that in mind, the model predictions seem valid.

SENSITIVITY ANALYSIS

The validation exercise of the previous section was carried out expending all possible effort to describe the experimental conditions and the material properties as completely as possible for the calculation model. To put the results obtained in a practical perspective, a sensitivity analysis has been carried out. The study focuses on how the materials' vapor permeabilities are described as functions of relative humidity. The purpose of this investigation is to get a grasp of how well predictions can be made by a building designer who usually would not have

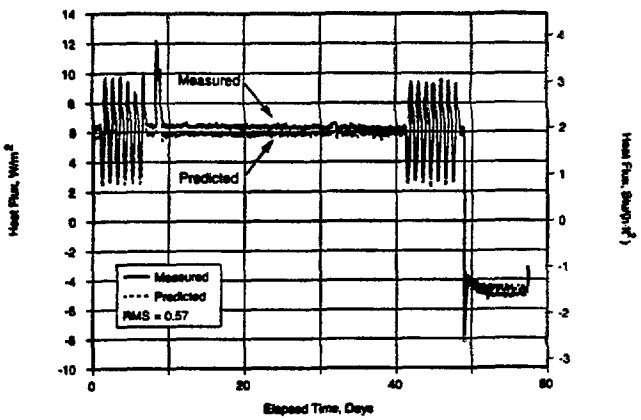

Figure 5 Comparison of measured and predicted heat fluxes throughout the entire test period, wall specimen A.

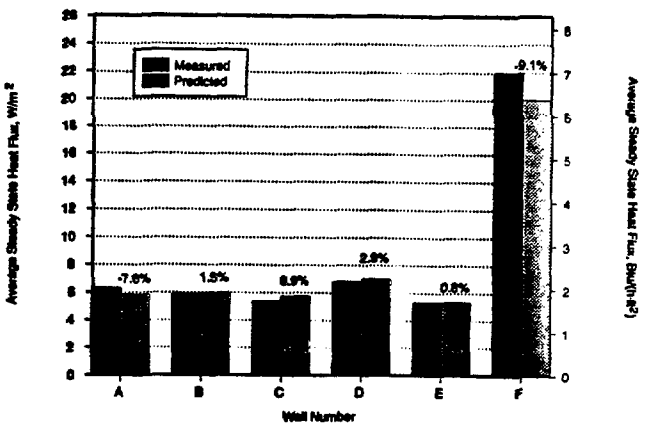

Figure 6 Comparison of measured and predicted average heat fluxes during the steady-state part of the test period, all wall specimens.

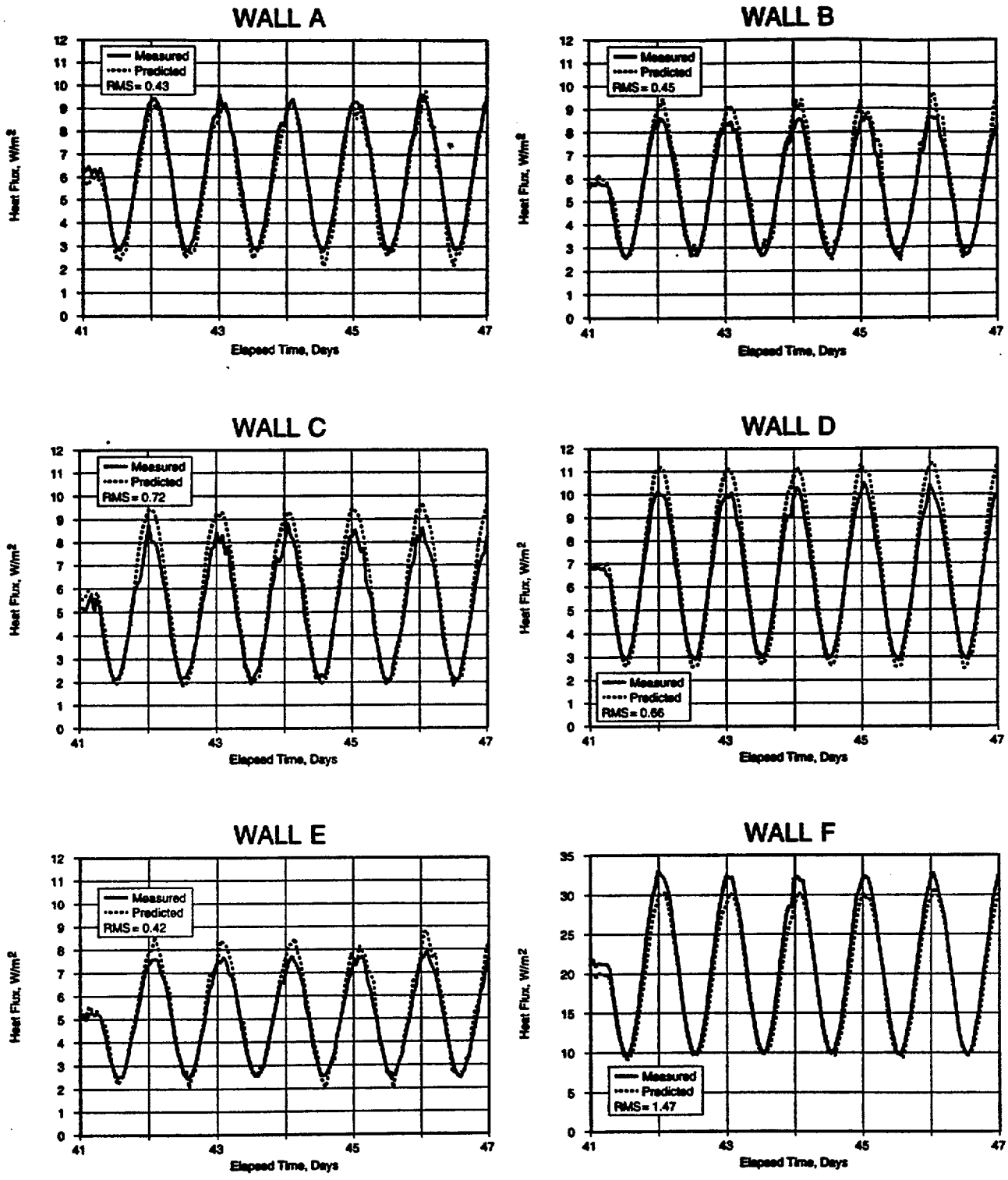

Figure 7 *Comparison of measured and predicted heat fluxes during the last of the two dynamic parts of the test period—all walls. Notice the different ordinate axis for Wall F.*

such detailed information on material properties available as in the validation exercise. Only wall A will be considered in this analysis.

To test the influence of how well the material properties are described, the model predictions used either of the following descriptions of the material properties.

- "Optimum"—For each material, the vapor permeability was given as a table that describes this property as a detailed function of relative humidity the way it was measured in the experiment (same condition as for the validation in the previous section).
- "Crude"—The vapor permeability as a function of relative humidity is given as two straight lines: A constant value up to 60% RH and a linear function of RH from 60% to 100%. Each of the two lines represents best-fit approximations to the "optimum" case in the RH domain it covers.
- "Constant"—The vapor permeability is given as a constant value over the full RH domain. In order to assign such a value for each material, a constant vapor permeability was determined using an absolute value technique on the basis of intermediate results from the optimum calculation:

$$\delta_p = \Delta x \frac{\Sigma|g_v|}{\Sigma|\Delta p_v|} \qquad (6)$$

where g_v = vapor flux through the material, kg/(m²·s) (lb/[ft²·h]).

Sums were taken over all time steps in the test period.

- "Engineer's choice"—This choice uses the permeability of the materials in the database that comes with the simulation program being used. The only similarity between materials in the experiment and in the database is their name and thus this is an arbitrary choice not utilizing any previous knowledge about the materials in the construction. It is meant to represent an engineer's choice in a design situation.

TABLE 7 **Vapor Permeabilities used in the Sensitivity Analysis (ng/m·s·Pa)**

Material	RH (%)	Optimum	Crude	Constant	Engineer
Sugar pine	60	1.05	0.495	2.37	1.50
	98	11.6	9.43		15.0
Glass-fiber	60	182	182	182	157
	98	182	182		157
Gypsum wallboard	60	63.8	63.8	63.8	23.6
	98	63.8	63.8		26.6

The vapor permeability of sugar pine in each of these cases is depicted in Figure 8. Sugar pine is the material among the ones in the experiment whose vapor permeability varies the most with the RH level. The vapor permeability at 60% and 98% RH is given in Table 7 for each of wall A's materials using any of the four ways to describe this function.

Figure 9 shows the measured moisture content on the inside of the sugar pine siding together with each of the predicted results. As can be seen, with either the case when a very detailed permeability function was used or a somewhat crude one, the resulting moisture contents track each other closely and correspond well with the measured result (RMS values around 1% by weight).

When a constant vapor permeability was used, there was a considerable increase in the deviation from the measured results (RMS more than 3% by weight). A result like this, however, depends very much on how the constant value is selected. In the case when permeability functions for seemingly similar materials from a database were used, there was also a noticeable deviation from

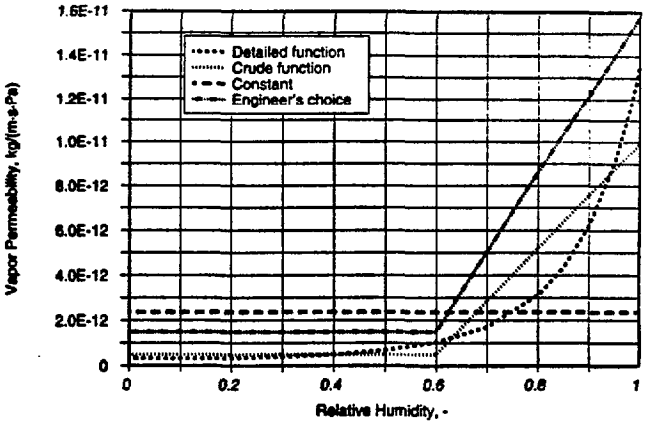

Figure 8 Different approaches to approximate the vapor permeability as a function of RH, here shown for sugar pine, the permeability of which varies the most with RH of the materials in the experiment.

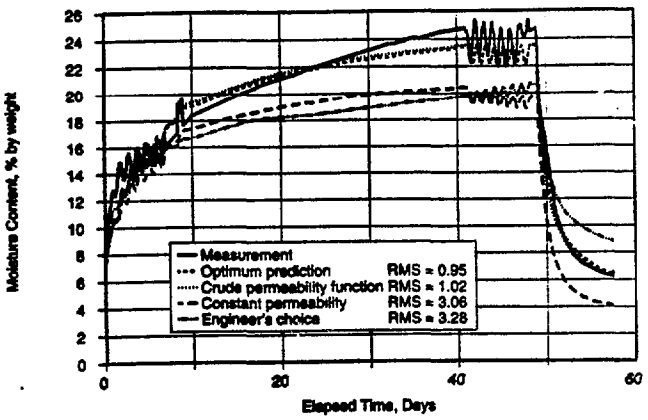

Figure 9 Comparison of the predicted moisture content of inside 3.2 mm of sugar pine of Wall A when different approaches are used to approximate the vapor permeability.

both the measured result and from the results of the more accurate predictions (RMS = 3.28).

In the last two cases, the deviations are large enough that they may lead a designer to make wrong conclusions about the moisture performance of the construction, e.g., if 20% moisture content by weight is the critical moisture content to avoid fungal attack of sugar pine.

To investigate the influence of numerical grid spacing on the results, test runs were carried out with a total of either 18 or 50 control volumes to compare with the use of 29 control volumes, as in the previous investigations. The solution for 18 control volumes had a 5% higher root-mean-squared error for the sugar pine's moisture content, while the RMS was 7% lower when 50 control volumes were used.

It must be emphasized that the results of this paper's analysis adhere strictly to the type of construction being examined, so one should be careful to draw general conclusions from this. It seems reasonable to state, nevertheless, that accurate material properties should always be procured before a computer prediction is carried out. It is preferred that these data be available in a functional form that accurately describes how they vary with important variables such as the humidity level. Different variations of the grid spacing should be tested in order to find a control volume size that gives a reasonable accuracy.

CALCULATION WITH GLASER METHOD

Since the Glaser method (Glaser 1959) is still common, it would make sense to apply this method to the type of construction analyzed in the paper. This has been done for wall A, using the boundary conditions of the steady winter periods, thermal conductivities from Table 5, and the constant vapor permeabilities of Table 7. The result is shown as a Glaser calculation scheme in Table 8.

It turns out that the Glaser method predicts that there is just barely no condensation in the construction. However, the relative humidity on the inside of the sugar pine is 99.7%. Using the sorption curve, Equation 3, and the coefficients for sugar pine from Table 2 gives an equilibrium moisture content of 26.5% by weight for the inside of the sugar pine. This corresponds well with the predicted and measured results toward the end of the long steady-state period of Figure 4. However, the Glaser method assumes steady-state conditions and does not provide any information on how long it would take to reach such an equilibrium. The transient calculation method gives a good prediction of this. Also, because the Glaser method does not consider the hygrothermal capacity of the materials, it will not be possible to use this method to simulate the periods with dynamic exposure. Finally, since the Glaser method requires constant material properties, it is up to the user to provide qualified estimates of these, whereas a transient simulation model will typically be able to approximate the variable nature of the properties.

CONCLUDING DISCUSSION

Models that can predict the hygrothermal behavior of composite building constructions are now becoming available to the research community as well as to building practitioners.

The computer model to calculate heat and moisture transfer that has been partially verified in this paper is able to predict moisture contents and heat flows with good accuracy when compared to results from an experimental study of lightweight wall constructions subjected to conditions in the hygroscopic region.

All the basic transport properties of the materials in the wall constructions were known from the experiment. This is unique for a full-scale experiment and makes the experiment well suited for validation purposes. This basic knowledge of the material properties and the experimental boundary conditions made a valid comparison between model and experiment possible.

A sensitivity analysis was carried out with the model for different situations with crude descriptions of the material properties as functions of relative humidity—or

TABLE 8 **Glaser Scheme to Calculate Vapor Pressure Distribution**

Layer	Thickness (m)	Thermal Resistance ($m^2 \cdot K/W$)	Vapor Resistance ($GPa \cdot m^2 \cdot s/kg$)	Temperature (°C)	Saturation Vapor Pressure (Pa)	Vapor Pressure (Pa)	RH (%)
Metering Chamber				21.2	2517	1259	50
Surface Resistances		0.12	0.07				
				20.5	2411	1249	51.8
Gypsum	0.0127	0.08	0.20				
				20.0	2338	1222	52.3
Glass-fiber	0.0813	1.83	0.45				
				9.2	1164	1160	99.7
Sugar pine	0.0191	0.22	8.06				
				7.9	1065	56	5.3
Surface Resistances		0.11	0.04				
Climate Chamber				7.2	1016	51	5

with selections from a database of properties of seemingly similar materials. The conclusion from this analysis should not be extended to other cases than the one analyzed in this paper. This analysis revealed that noticeable differences in the calculation results could result if the material properties are not described accurately. It also seems to be beneficial that these properties are described as some function of the humidity level. However, it does not seem necessary to spend a great amount of effort to optimize the functional form of such a dependency.

For extended steady-state conditions, results with the Glaser method and with the transient model correspond well with one another. However, the Glaser method does not provide any information about the dynamic hygrothermal behavior of such a wall.

So is it safe to let transient simulation programs for combined heat and moisture transfer be used by those other than the developers? This, probably, is still a question that can only be answered with some controversy. This paper has shown that for a particular case—a lightweight insulated wall exposed to conditions in the hygroscopic regime—good predictions can be obtained but also that small changes in model input may change the calculation results noticeably. Users of such models should, at a minimum, have a good knowledge of the working of the model, the required input parameters, and, perhaps most important, the limitations of the model.

REFERENCES

ASHRAE. 1993. *1993 ASHRAE handbook—Fundamentals.* Atlanta, Ga.: American Society of Heating, Refrigerating and Air-Conditioning Engineers, Inc.

ASTM. 1993. ASTM Test method C 177, Thermal insulation, environmental acoustics. *Annual Book of ASTM Standards,* vol. 04.06. Philadelphia, Pa.: American Society for Testing and Materials.

Burch. D.M., and W.C. Thomas. 1994. MOIST—A PC program for predicting heat and moisture transfer in building envelopes. NIST Special Publication 853. Gaithersburg, Md.: National Institute of Standards and Technology.

Burch, D.M., W.C. Thomas, and A.H. Fanney. 1992. Water vapor permeability measurements of common building materials. *ASHRAE Transactions* 98(2).

Chlusov, I.E. 1958. On the calculation of moisture in roof constructions. (Original in Russian). *CIB Conference on Flat Roofs,* June 9-11, Stockholm.

Duff, J.E. 1968. Moisture distribution in wood-frame walls in winter. *Forest Products Journal* 23(1).

Glaser, H. 1959. Graphisches Verfahren zur Untersuchung von Diffusionsvorgänge. *Kältetechnik* 10: 345-349.

Greenspan, L. 1977. Humidity fixed points of binary saturated aqueous solutions. *Journal of Research, National Bureau of Standards* 81A: 89-96.

Hens, H., and A. Janssens. 1993. Enquiry on HAMCaT codes. *Energy Conservation in Buildings and Community Systems Programme.* Annex 24. Heat, Air and Moisture Transfer in Insulated Envelope Parts. International Energy Agency,

Kießl, K. 1983. *Kapillarer und dampfförmiger Feuchtetransport in mehrschichtigen Bauteilen.* Universität-Gesamthochschule-Essen.

Kohonen, R. 1994. A method to analyze the transient hygrothermal behavior of building materials and components. Publication 21. Espoo: Technical Research Centre of Finland.

Künzel, H.M. 1994. Verfahren zur ein- und zweidimensionalen Berechnung des gekoppelten Wärme und Feuchtetransport in Bauteilen mit einfachen Kennwerten. Ph.D. thesis. Universität Stuttgart.

Kyle, D.M., and A. Desjarlais. 1994. Assessment of technologies for constructing self-drying low-slope roofs. ORNL/CON-380. Oak Ridge, Tenn.: Oak Ridge National Laboratory.

Luikov, A.V. 1966. *Heat and mass transfer in capillary-porous bodies.* London: Pergamon Press.

Nielsen, A.F. 1974. Moisture distributions in cellular concrete during heat and moisture transfer. Ph.D. thesis. Thermal Insulation Laboratory, Technical University of Denmark.

Pedersen, C.R. 1990. Combined heat and moisture transfer in building constructions. Ph.D. thesis. Thermal Insulation Laboratory, Technical University of Denmark.

Pedersen, C.R. 1991. Classification of model MATCH. IEA, Energy Conservation in Buildings and Community Systems Programme, Annex 24. Report T1-DK-91/01.

Pedersen, C.R., and G. Courville. 1991. A computer analysis of the annual thermal performance of a roof system with slightly wet fibrous glass insulation under transient conditions. *Journal of Thermal Insulation* 15: 110-136.

Pedersen, C.R., T.W. Petrie, G.E. Courville, A.O. Desjarlais, P.W. Childs, and K.E. Wilkes. 1992. Moisture effects in low slope roofs: Drying rates after water addition with various vapor retarders. ORNL/CON-308. Oak Ridge, Tenn.: Oak Ridge National Laboratory.

Philip, J.R., and D.A. de Vries. 1957. Moisture movement in porous materials under temperature gradients. *Transactions, American Geophysical Union* 38: 222-232.

Richards, R.F., D.M. Burch, and W.C. Thomas. 1992. Water vapor sorption measurements of common building materials. *ASHRAE Transactions* 98(2).

Threlkeld, J.L. 1970. *Thermal environmental engineering,* pp. 196-198. New York, N.Y.: Prentice-Hall, Inc.

van der Kooi, J. 1971. Moisture transport in cellular concrete roofs. Ph.D. thesis. Delft, the Netherlands: Uitgeverij Waltman.

Zarr, R.R., D.M. Burch, T.K. Faison, C.E. Arnold, and M.E. O'Connell. 1987. Calibration of NBS calibrated hot box. *Journal of Testing and Evaluation* 15(3).

Zarr, R.R., D.M. Burch, and A.H. Fanney. 1995. Heat and moisture transfer in wood-based wall construction: Measured versus predicted. Building Science Series 177. Gaithersburg, Md.: National Institute of Standards and Technology.